Protein Interactions

Modulation of Compactness and Long-Range Interactions of Unfolded Lysozyme by Single Point Mutations**

*Julia Wirmer, Christian Schlörb, Judith Klein-Seetharaman, Ryoma Hirano, Tadashi Ueda, Taiji Imoto, and Harald Schwalbe**

Non-native states of proteins are not only the starting point of protein folding, but they are also implied in misfolding, transport through membranes, protein turnover, and degradation processes. An increasing number of intrinsically unstructured or natively unfolded proteins have been identified, some of which exert their function in this unstructured state.[1] Unlike the native state of a protein, non-native states cannot be described by a single conformation, but rather they exist as an ensemble of rapidly interconverting conformers. The individual members of this ensemble may differ substantially in their structural and dynamical properties, and different parts of the polypeptide chain may change conformation at different rates.[2] Previous studies showed that the conformational ensemble samples the preferred regions of the Ramachandran φ,ψ space. This sampling, however, can be restricted by varying degrees of residual structure: Secondary structure elements in unfolded proteins have been identified in a large number of proteins by comparison of local NMR parameters with values expected in a random coil.[3–9] In contrast, the identification of longer-range interactions is not as straightforward. The conformational averaging in unfolded proteins renders it only possible to detect short- or medium-range NOE (nuclear Overhauser effect) interactions. Long-range interactions can only be identified by using mutations in combination with NMR spectroscopic techniques such as relaxation rates,[10] spin labels, residual dipolar couplings, or diffusion rates.

NMR spectroscopic studies of non-native states of hen lysozyme have revealed the existence of clusters of residual secondary structure.[6,10] The locations of these clusters strongly correlate with clusters of hydrophobic amino acids, a correlation that was also observed for other proteins.[11–13] These hydrophobic clusters in non-native lysozyme are stabilized by long-range interactions.[10] However, the extent to which each of these clusters contributes to the stability of the entire conformational ensemble is an important, yet unanswered question. Herein we study the effects of point mutations in the major hydrophobic clusters on the ensemble of structures that are present in unfolded lysozyme. The results show that nonconservative single point mutations in the hydrophobic clusters dramatically change the overall compactness of non-native lysozyme by the modulation of long-range interactions between hydrophobic clusters.

The distribution of hydrophobic amino acids in the lysozyme sequence is shown in Figure 1a. The hydrophobicity predictions were fitted to six distinct clusters with maximal hydrophobicity around (1) C6, (2) W28, (3) L56, (4) L83, (5) W108, and (6) W123 (C = cysteine, W = tryptophan, and L = leucine) by using Gaussian models. Mapping of the hydrophobic clusters onto the structure of lysozyme[14] showed that the clusters ultimately result in the hydrophobic cores of the α- and β-domains of the protein. The location of the hydrophobic clusters has an impact on the unfolded states: 1) Experimentally determined folding-core residues map to the central parts of clusters 1–4.[15–18] 2) Residual non-random secondary structures tend to cluster at similar positions (Figure 2A). 3) The positions of hydrophobic clusters overlap to a remarkable extent with the average restrictions in conformational space in unfolded ensembles of lysozyme as identified by relaxation rate measurements (Figure 3a). In contrast to the excellent correlation between the positions of the experimentally determined clusters of residual structure and those of all of the hydrophobic clusters, the intensities of the clusters do not match well for clusters 1 and 4, for which barely elevated relaxation rates were found. Interestingly, these two clusters are the only two regions of predicted increased hydrophobicity (Figure 1a) that do not contain tryptophan residues.

We investigated the effects of two types of single point mutations on the compactness and interaction of clusters: 1) replacement of tryptophan residues with either tyrosine (Y) or glycine (G) moieties (W62Y/G) and 2) replacement of a central amino acid, with emphasis on tryptophan units, in clusters 1, 3, 5, and 6 with glycine (A9G, W62G, W111G, and W123G (see Figure 1b). The Trp28 mutant protein was too unstable for sufficient amounts of protein to be obtained and was therefore not investigated. Cluster 4 was not studied because the wild-type (WT) protein already displays very little deviation from the random coil in this region. To obtain a model system for the study of non-native states of lysozyme, WT and mutant lysozyme were denatured, the four native

[*] J. Wirmer, C. Schlörb, J. Klein-Seetharaman, Prof. Dr. H. Schwalbe
Institute for Organic Chemistry and Chemical Biology
Center for Biomolecular Magnetic Resonance
Johann Wolfgang Goethe University Frankfurt
Marie-Curie-Strasse 11, 60439 Frankfurt (Germany)
Fax: (+49) 69-798-29515
E-mail: schwalbe@nmr.uni-frankfurt.de
J. Wirmer
Department of Chemistry
Massachusetts Institute of Technology
Cambridge MA 02139 (USA)
J. Klein-Seetharaman
Department of Pharmacology, University of Pittsburgh
School of Medicine
Pittsburgh PA 15261 (USA)
R. Hirano, T. Ueda
Graduate School of Pharmaceutical Science
Kyushu University
Fukuoka 812-8582 (Japan)
T. Imoto
Department of Applied Microbial Technology
Faculty of Engineering
Sojo University
Ikeda 4-22-1, Kumamoto 860-0082 (Japan)

[**] We thank the Fonds der Chemischen Industrie (Germany) for stipends to J.W. and C.S., and the State of Hessen for financial support.

  DOI: 10.1002/ange.200460907

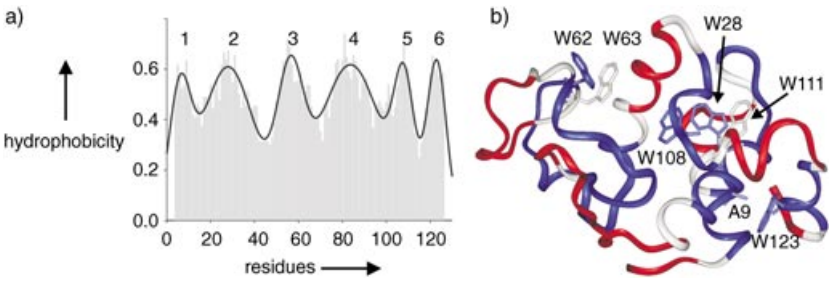

Figure 1. a) Distribution of hydrophobicity in lysozyme: normalized values (0–1) of hydrophobicity according to the scheme of Abraham and Leo;[32] Gaussian least-squares fitting of hydrophobic clusters is shown as a black line, and the clusters are numbered 1–6. b) Positions of Ala9 (A9) and tryptophans (W) in the native state: the crystal structure of lysozyme (deposited in the Protein Data Bank (193L) [14]) shown is colored according to the hydrophobicity values that were obtained from the Gaussian fit (red: nonhydrophobic (0–0.46); blue: hydrophobic (0.52–1); for comparison: glycine = 0.49).

disulfide bonds were reduced and methylated (indicated by S^{Me}), and the products were studied in water at pH 2, at which hydrogen exchange is slowed down. This variant of lysozyme remained unfolded in the absence of denaturant even at near-native conditions (pH 6, data not shown), but measurements were carried out at pH 2 owing to the slow rates of amide exchange.

NMR H^N, H^α, and C^α chemical shifts were used for secondary-structure prediction.[19,20] In WT-S^{Me}, all the chemical shift values were close to those of the random coil which indicates that the reduced protein is unstructured. Remaining small perturbations in the chemical shift values of H^N and H^α atoms of WT-S^{Me}, relative to chemical shifts measured in small unstructured peptides,[21,22] are shown in Figure 2 A, parts a and b, respectively. Deviations were found for Gly 22 (H^N), for Val 29 and Cys-S^{Me} 30 (both H^α), around Trp 62/Trp 63 (R61 (H^α); W62, W63, and C64 (H^N)), and around Trp 108/Trp 111 (V109, R112 (H^α); W111, N113, and R114 (H^N); (V = valine, R = arginine). The degree of helicity was estimated by a comparison of the measured C^α chemical shifts[23] with those values expected for the random coil[19] and those derived statistically for α-helices.[24] High induced helicity was found for residues 8–12 and around Trp 108/Trp 111. A mean degree of helicity of 12.3 % was calculated (Figure 2 A, part c). This value is in excellent agreement with a global value of 14.4 % derived from circular dichroism (CD) spectroscopy measurements (Figure 2 A, part d).

The effect of the replacement of a single amino acid, namely Trp 62 in W62G and W62Y in cluster 3, and the mutations A9G, W111G, and W123G, on the H^α chemical shift is shown in Figure 2, B and C, respectively. The data are presented as correlations between the chemical shift values of H^α atoms in the single point mutants with those in WT-S^{Me}. The H^α atoms of the conservative mutations W62Y and A9G

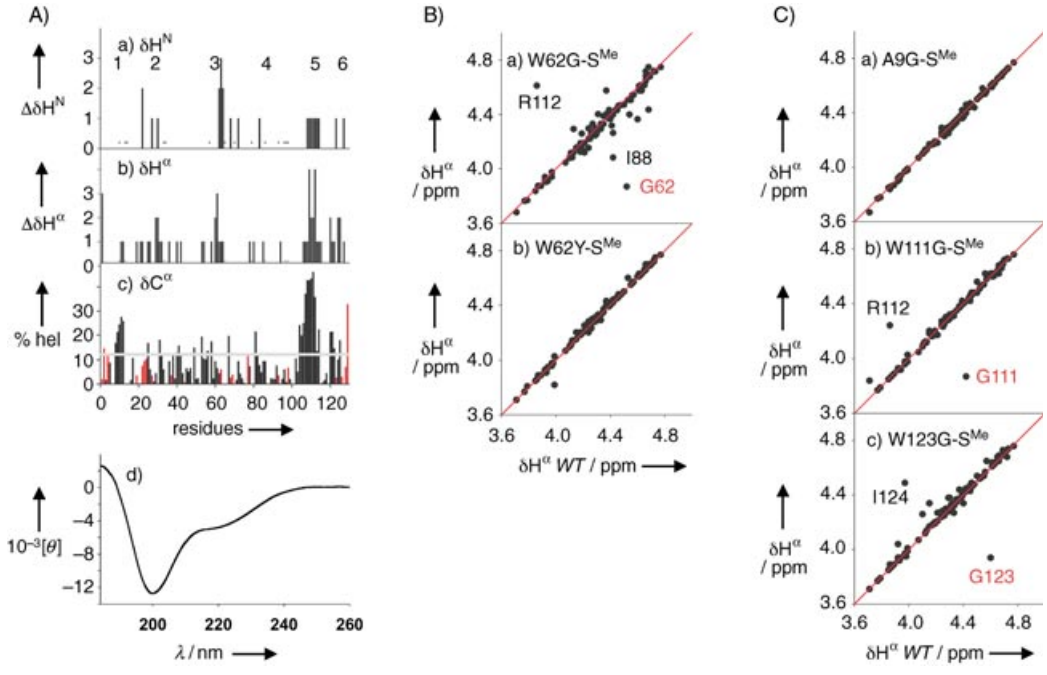

Figure 2. Residual secondary structure in unfolded lysozyme. A) Normalized values of the differences between the chemical shifts of a) H^N and b) H^α centers in WT-S^{Me} relative to those in the random coil ($\Delta\delta = \delta exp - \delta rc$).[6] Residues for which chemical shifts could not be determined are indicated by an asterisk. c) The percentage of residual helicity (% hel) in WT-S^{Me} are shown as black (positive) and red (negative) vertical bars as a function of the number of residues. A mean value of the induced positive helicity of 12.3 % is indicated by the horizontal line. d) CD spectrum of WT-S^{Me} ($[\theta]$/deg cm^2 mol^{-1}); a helicity of 14.4 % was estimated by using the approach of Rohl and Baldwin.[36] Correlation between the chemical shift values of Hα in B) W62G-S^{Me} and W62Y-S^{Me}, and C) A9G-S^{Me}, W111G-S^{Me}, and W123G-S^{Me} in WT-S^{Me} with those of the wild-type (WT) protein; strongly deviating residues are indicated (black) as well as the mutated amino acids (red).

display chemical shift values that are virtually identical to those of the WT. The largest deviations in these correlations were found for W62G, which has longer-range effects in particular on R112 and I88 (I = isoleucine), which are distant from the point of mutation at position W62. W111G and W123G show predominantly local deviations, including the mutation site and immediate neighbors in the sequence. However, overall, the deviations of the chemical shifts of the protons from the mutants relative to those of the WT proteins are small for all mutants, even for the regions around the chosen mutation sites which have correlation coefficients that range between 0.996 (A9G) and 0.849 (W62G). We conclude that local regions of residual secondary structure are not disturbed by the mutations.

Because non-native states of proteins are the "averages" of interconverting fluctuating conformations, a single set of tertiary contacts in the unfolded state cannot be determined. However, averaged restrictions in conformational space were measured by the ^{15}N NMR spectroscopic transverse relaxation rates (R_2) and the diffusion-derived hydrodynamic radius (R_h). R_h is determined by the diffusion of the polypeptide chain and is therefore averaged over the ensemble of conformers. R_2 relaxation rates depend on the anisotropic rotational correlation time (τ_c) and are sensitive to motions of the backbone on the subnanosecond timescale and also to slow conformational exchange on the millisecond timescale.[25–27] Previously, by comparison of R_2 and $R_{1\rho}$, we showed that the effect of slow conformational exchange on R_2 rates in WT-S^{Me} is negligible.[6] In the fully unfolded state of a protein, the internal motions can be described as arising from segmental motions, and the profile of relaxation rates for the random coil R_2^{rc} can be predicted from polymer theory,[28] which is independent of the molecular weight. In compact unfolded states, the interactions of some segments lead to deviations from random-coil behavior. Therefore, the extent of deviation from the random-coil model can be used to delineate long-range, tertiary interactions.[6,10]

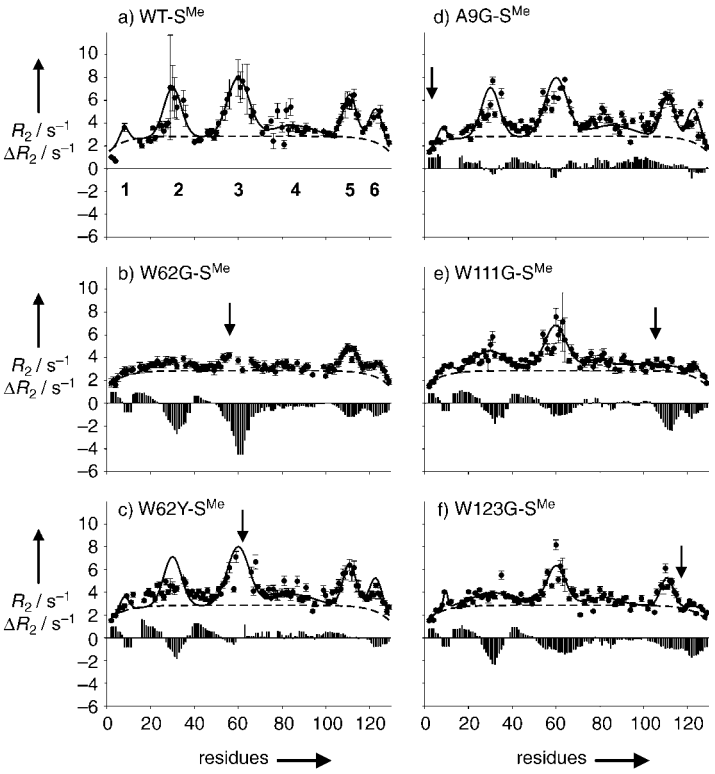

Figure 3. Residual tertiary interactions in unfolded lysozyme (hydrophobic clusters are indicated by numbers 1—6). a–f) ^{15}N R_2 relaxation rates in WT-S^{Me} and W62G-S^{Me}, W62Y-S^{Me}, A9G-S^{Me}, W111G-S^{Me}, and W123G-S^{Me}, respectively. The experimental rates are shown as scatter plots, whereas the rates fitted by a segmental motion model and expected for a random coil with R_2^{rc} ($R_{int} = 0.2\ s^{-1}$ and $\lambda_0 = 7$) are shown as dashed lines; black lines show the Gaussian fits for WT-S^{Me} (a, c, and d), W111G-S^{Me} (e), and W123G-S^{Me} (f). Deviations of R_2 relaxation rates of the mutants from relaxation rates of WT-S^{Me} ($\Delta R_2 = R_2$(mutant-S^{Me}) $- R_2$(WT-S^{Me})) were averaged over 7 residues and are shown as bars.

Figure 3 shows the heteronuclear ^{15}N transverse relaxation rates (R_2^{exp}) of WT-S^{Me} and the mutants that were studied. For comparison, the rates that were determined previously[10] for WT-S^{Me} and W62G-S^{Me} are also reproduced. Increased relaxation rates in WT-S^{Me} coincide with the six hydrophobic clusters and the positions of residual secondary structure, which were identified from measurements of the chemical shift values. Replacement of Trp62 by glycine essentially abolishes not only its own cluster 3 (Figure 3b), but also clusters 1–4 and diminishes clusters 5 and 6.[10] Long-range interactions between Trp62 and the other hydrophobic clusters of lysozyme therefore must be present and stabilized by the tryptophan moiety. To test if this property of Trp62 is unique to tryptophan or whether it may be more generally attributable to aromatic amino acids, the effect of replacing Trp62 by tyrosine on the relaxation behavior of unfolded lysozyme was studied (see Figure 3c). The W62Y mutation has a very minor effect on the relaxation properties of WT-S^{Me} relative to W62G-S^{ME}. This result suggests that aromatic residues play an important role in the stabilization of long-range interactions in unfolded states of lysozyme. A9G-S^{Me} displays even more similar properties to WT-S^{Me}, and there is not even an effect on its own cluster, cluster 1. The size and the position of the hydrophobic clusters remain virtually identical which indicates that Ala9 is not important in the stabilization of the hydrophobic core.

In contrast, the replacement of tryptophan residues at positions 111 and 123 led to significant results. Upon replacement of Trp111 (cluster 5) by glycine, the cluster in which the mutation is located, namely cluster 5, disappeared entirely and cluster 6 also decreased significantly in intensity. A loss in the intensity of cluster 2 (surrounding Trp28) was observed as well as a very small decrease in the intensity of cluster 3 (surrounding Trp62 and Trp63). Similarly, when Trp123 at the C terminus (cluster 6) was changed to glycine, the cluster around the mutation site essentially disappeared, and the intensities of clusters 2, 3, and 5 were lessened. The effect of the replacement in W123G is less significant than that of W111G, as seen by the complete loss of cluster 5 in W111G-S^{Me} but not in W123G-S^{Me}. The largest changes in the

distribution of R_2 relative to WT-S^{Me} were observed with W62G-S^{Me}.

The decrease in the R_2 values upon single point mutations indicates that changes in the conformational ensembles of lysozyme occurred. Thus, it is predicted that those point mutations which cause a change in relaxation profiles can also cause a change in the compactness of the average unfolded state. A loss of conformational restriction in one or more of the hydrophobic clusters would increase the overall propensity for extended states in the ensemble. This hypothesis was tested directly by measuring the averaged hydrodynamic radii R_h from NMR diffusion measurements of the different reduced and methylated proteins. WT-S^{Me} and W123G-S^{Me} diffuse quickly, W111G-S^{Me} diffuses at intermediate velocity, and W62G-S^{Me} diffuses the slowest. Figure 4a shows the

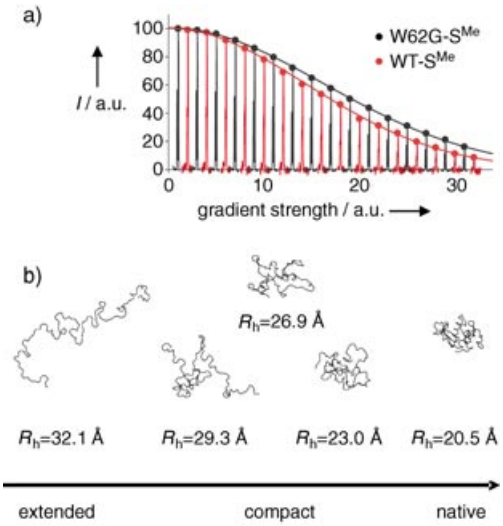

Figure 4. Changes in compactness as a result of point mutations. a) Diffusion experiments that were used to determine the hydrodynamic radii (R_h). The intensity of the NMR signal is shown as a function of gradient strength (g) for WT-S^{Me} (black) and W62G-S^{Me} (red). The decay of the signal was fitted to a function of the form $I = A e^{-Dg^2}$. R_h values were calculated from decay rates (D, see Experimental Section). b) Randomly chosen conformations with the amino acid sequence of lysozyme in relation to their hydrodynamic radius. Conformations with increasing (experimental) R_h values are shown. The radii of different conformations were calculated using the program Hydropro.[40]

diffusion measurements for WT-S^{Me} and W62G-S^{Me}. The R_h values that were calculated from the diffusion rates (see the Experimental Section) are 26.9 ± 0.6, 25.4 ± 1.2, 29.3 ± 1.3, and 32.1 ± 0.6 Å for WT-S^{Me}, W123G-S^{Me}, W111G-S^{Me}, and W62G-S^{Me}, respectively (these values are concentration-independent (40–60 μM)). All R_h values are considerably larger (at least 25%) than the R_h value of folded lysozyme ($R_h = 20.5$ Å)[29] which indicates the extended nature of the reduced and methylated states. However, the overall average shape of the ensemble of conformers markedly varies with the position of the single point mutations in the different hydrophobic clusters. Whereas similar hydrodynamic radii were measured for WT-S^{Me} and W123G-S^{Me}, the hydrodynamic radius of W111G-S^{Me} was larger ($R_h = 29.3 \pm 1.3$ Å) and that of the W62G-S^{Me} mutant was the largest ($R_h = 32.1 \pm 0.6$ Å; see Figure 4b). Conformations were calculated by unbiased molecular dynamics simulations. As one can see, the R_h value of 32.1 Å for W62G-S^{Me} corresponds to a very extended, almost linear conformation, which is consistent with the essentially random-coil behavior observed for the relaxation rates of this mutant (Figure 3b). The radii observed for the other mutants correspond to rather compact states with a clear presence of tertiary contacts. These states are much closer to the native state with a R_h value of 20.5 Å than the very extended conformation that has a R_h value of 32.1 Å.

The comparison between experimental NMR parameters and those expected for a true random coil show that there are six areas that display strong deviations from random-coil behavior in WT-S^{Me}. The observed hydrodynamic radius of 26.9 ± 0.6 Å indicates that the average conformations in WT-S^{Me} are rather compact (Figure 4b) which supports the presence of extensive tertiary contacts in the unfolded state. These contacts are both nativelike and non-nativelike. Non-native contacts between cluster 3—around Trp62 and Trp63, which form part of the β-domain in the native structure (see also Figure 1b)—and the clusters 1, 2, and 4, which form the α-domain, must be present because deviations from random-coil relaxation behavior are decreased in the W62G mutant. Breakage of these long-range interactions results in a dramatic increase by 12% in the measured R_h values from WT-S^{Me} to W62G-S^{Me} which reflects a shift towards very extended conformations (Figure 4b). The presence of native-like contacts is suggested by the effect of the W123G mutation which simultaneously diminishes clusters 6 and 2, indicating nativelike contacts between Trp123 and sites at or around Trp28. The importance of native-like contacts is consolidated by the central role of the Trp111 interactions in WT-S^{Me}. Disruption of the contacts between Trp111 and the cluster that surrounds Trp28 by the W111G mutation results in a large increase in R_h of ≈9%. Tryptophan residues or aromatic residues in general apparently play a special role in the stabilization of contacts in compact states of unfolded lysozyme. A comparison of the effects of replacing Trp62 with glycine and with tyrosine shows that there are little changes in the relaxation behavior of W62Y-S^{Me} relative to WT-S^{Me}, in contrast to W62G-S^{Me}, which shows the strongest deviations from WT-S^{Me}. Aromatic residues play a significant role in the organization of nearby residues into arrangements that have restricted motions compared to a completely unfolded polypeptide chain.

Point mutations induce a shift in the distribution of conformers from compact to more-extended states to differing degrees depending on the location of the mutation with respect to the hydrophobic clusters present. Such changes are expected to result in differences in the rates at which folding and misfolding events take place. Extended structures will clearly have different propensities, for example, in the formation of disulfide bonds. Similarly, the time that is needed for an extended stretch of amino acids within the protein sequence to rearrange into another extended or into a more-compact state will be affected by the change in compactness induced by the different mutations.

Experimental Section

Hydrophobicity calculations were performed with the 'protscale' tool from the ExPAsy (Expert Protein Analysis System)[30,31] molecular biology server (http://us.expasy.org/cgi-bin/protscale.pl) by using the Abraham and Leo scale.[32] A window size (i.e., length of the interval used for profile computation) of 7 was used, and the weight at the edge of the window was set to 100%; the degrees of hydrophobicity shown were normalized from 0–1. Centres of elevated regions were identified by the fitting of Gaussian clusters to the data with the program SigmaPlot.

The construction of single point mutants of hen egg-white lysozyme, the expression and purification of ^{15}N-labelled protein in the yeast *Pichia pastoris*,[33,34] and the methylation of reduced lysozyme[35] were performed according to reported methods.

CD spectra were recorded as described,[23] and the mean helix content was calculated by using the approach of Rohl and Baldwin.[36] NMR experiments were recorded at 293 K on a four-channel Bruker DRX600 spectrometer, which was equipped with a cryo-probe, with *z*-gradients. Samples of the proteins (≈60–100 μM) were prepared in water (10% D_2O, pH 2). 3D NOESY–HSQC (hetero-nuclear single quantum coherence) experiments were recorded and analyzed as previously reported.[6] Perturbations of the chemical shifts of H^N and H^α atoms were derived as previously described.[6] Residual helicity is defined by the percentage of induced helicity (% hel), which is obtained from a comparison of the C^α chemical shifts in WT-S^{Me} (C^α_{exp}) with the C^α chemical shifts in the random coil (C^α_{rc})[19,20,23] and those derived statistically for α-helices (C^α_{hel}),[24] according to Equation (1):

$$\%\ \text{hel} = 100\,\frac{\delta C^\alpha_{exp} - \delta C^\alpha_{rc}}{\delta C^\alpha_{hel} - \delta C^\alpha_{rc}} \tag{1}$$

Diffusion measurements were performed using 40–60 μM protein in D_2O at pH 2 (corrected for D_2O),[37] with 1,4-dioxane (200–300 μM) as internal standard (hydrodynamic radius: 2.12 Å; it has been shown that dioxane does not interact with proteins[38]). PFG (pulse field gradient)-NMR diffusion measurements were performed as reported.[29,38,39] Hydrodynamic radii (R_h) were calculated from the decay rates derived from NMR spectra by using Equation (2), in which D_{diox} and D_{prot} are the decay rates of dioxane and the protein, respectively.

$$R_h^{prot} = \frac{D_{diox}}{D_{prot}} R_h^{diox} \tag{2}$$

It was reported that the aggregation of methylated lysozyme (WT-S^{Me}), which is in exchange with the unfolded form, is observed as an increase in the apparent R_h for concentrations of the protein of 0.2–0.25 mM.[29] However, here, at concentrations of the protein of 40–60 μM for each mutant, R_h remained constant, which excludes aggregation processes. Predicted hydrodynamic radii (Figure 4) were calculated from the structures by using the program Hydro-pro.[40]

Transverse relaxation rates R_2 were measured and analyzed as previously reported.[6] Relaxation rates in an extended polypeptide can be described by a simple model, which is derived from polymer theory[28] and is referred to as the segmental motion model. The segmental model assumes that the influence of the neighboring residues decays exponentially as the distance (in terms of the number of peptide bonds) from a given residue increases.[6] Therefore, R_2 relaxation rates of unfolded proteins can be fitted to Equation (3), in which R_{int} is the intrinsic relaxation rate, which depends also on the temperature and viscosity of the solution, λ_0 is the persistence length of the polypeptide chain (in terms of the numbers of residues), and N is the total chain length of the polypeptide:

$$R_2^{rc}(i) = R_{int} \sum_{j=1}^{N} e^{-\frac{|i-j|}{\lambda_0}} \tag{3}$$

Experimental R_2 rates of lysozyme show that there are regions of positive deviation from the segmental model that can be fitted by Gaussian distributions. Thus, a model is proposed that includes two components: the segmental motion part [Eq. (3)] and a Gaussian term, as shown in Equation (4).

$$R_2^{exp}(i) = R_{int} \sum_{j=1}^{N} e^{-\frac{|i-j|}{\lambda_0}} + \sum_{cluster} R_{cluster}\, e^{-\left(\frac{i-x_{cluster}}{2\lambda_{cluster}}\right)^2} \tag{4}$$

These Gaussian clusters are characterized by the position of the cluster in the protein (residue number) $x_{cluster}$, the width of the cluster $\lambda_{cluster}$, and a distinct relaxation rate for each cluster $R_{cluster}$.

Received: June 8, 2004

Keywords: biophysics · lysozyme · mutagenesis · NMR spectroscopy · protein folding

[1] P. Tompa, *Bioessays* **2003**, *25*, 847.
[2] L. J. Smith, K. M. Fiebig, H. Schwalbe, C. M. Dobson, *Folding Des.* **1996**, *1*, R95.
[3] F. J. Blanco, L. Serrano, J. D. Forman-Kay, *J. Mol. Biol.* **1998**, *284*, 1153.
[4] D. Shortle, M. S. Ackerman, *Science* **2001**, *293*, 487.
[5] D. Shortle, C. Abeygunawardana, *Structure* **1993**, *1*, 121.
[6] H. Schwalbe, K. M. Fiebig, M. Buck, J. A. Jones, S. B. Grimshaw, A. Spencer, S. J. Glaser, L. J. Smith, C. M. Dobson, *Biochemistry* **1997**, *36*, 8977.
[7] K. M. Fiebig, H. Schwalbe, M. Buck, L. J. Smith, C. M. Dobson, *J. Phys. Chem.* **1996**, *100*, 2661.
[8] K. B. Wong, S. M. Freund, A. R. Fersht, *J. Mol. Biol.* **1996**, *259*, 805.
[9] M. A. Lietzow, M. Jamin, H. J. Jane Dyson, P. E. Wright, *J. Mol. Biol.* **2002**, *322*, 655.
[10] J. Klein-Seetharaman, M. Oikawa, S. B. Grimshaw, J. Wirmer, E. Duchardt, T. Ueda, T. Imoto, L. J. Smith, C. M. Dobson, H. Schwalbe, *Science* **2002**, *295*, 1719.
[11] D. Neri, M. Billeter, G. Wider, K. Wuthrich, *Science* **1992**, *257*, 1559.
[12] G. Saab-Rincon, P. J. Gualfetti, C. R. Matthews, *Biochemistry* **1996**, *35*, 1988.
[13] I. J. Ropson, C. Frieden, *Proc. Natl. Acad. Sci. USA* **1992**, *89*, 7222.
[14] M. C. Vaney, S. Maignan, M. RiesKautt, A. Ducruix, *Acta Crystallogr. Sect. D* **1996**, *52*, 505.
[15] A. Miranker, S. E. Radford, M. Karplus, C. M. Dobson, *Nature* **1991**, *349*, 633.
[16] M. Buck, S. E. Radford, C. M. Dobson, *J. Mol. Biol.* **1994**, *237*, 247.
[17] S. E. Radford, C. M. Dobson, P. A. Evans, *Nature* **1992**, *358*, 302.
[18] D. P. Nash, J. Jonas, *Biochemistry* **1997**, *36*, 14375.
[19] D. S. Wishart, B. D. Sykes, *J. Biomol. NMR* **1994**, *4*, 171.
[20] D. S. Wishart, B. D. Sykes, F. M. Richards, *Biochemistry* **1992**, *31*, 1647.
[21] D. S. Wishart, C. G. Bigam, A. Holm, R. S. Hodges, B. D. Sykes, *J. Biomol. NMR* **1995**, *5*, 67.
[22] S. Schwarzinger, G. J. Kroon, T. R. Foss, J. Chung, P. E. Wright, H. J. Dyson, *J. Am. Chem. Soc.* **2001**, *123*, 2970.
[23] C. Schlörb, C. Richter, K. Ackermann, J. Wirmer, H. Schwalbe, unpublished results.
[24] H. Zhang, S. Neal, D. S. Wishart, *J. Biomol. NMR* **2003**, *25*, 173.

[25] G. Wagner, *Curr. Opin. Struct. Biol.* **1993**, *3*, 748.
[26] G. Lipari, A. Szabo, *J. Am. Chem. Soc.* **1982**, *104*, 4559.
[27] G. Lipari, A. Szabo, *J. Am. Chem. Soc.* **1982**, *104*, 4546.
[28] A. Allerhand, R. K. Hailstone, *J. Chem. Phys.* **1972**, *56*, 3718.
[29] D. K. Wilkins, S. B. Grimshaw, V. Receveur, C. M. Dobson, J. A. Jones, L. J. Smith, *Biochemistry* **1999**, *38*, 16424.
[30] R. D. Appel, A. Bairoch, D. F. Hochstrasser, *Trends Biochem. Sci.* **1994**, *19*, 258.
[31] A. Bairoch, R. D. Appel, M. C. Peitsch, *Protein Data Bank Q. Newslett.* **1997**, *81*, 5.
[32] D. J. Abraham, A. J. Leo, *Proteins Struct. Funct. Genet.* **1987**, *2*, 130.
[33] S. Mine, T. Ueda, Y. Hashimoto, Y. Tanaka, T. Imoto, *FEBS Lett.* **1999**, *448*, 33.
[34] S. Mine, S. Tate, T. Ueda, M. Kainosho, T. Imoto, *J. Mol. Biol.* **1999**, *286*, 1547.
[35] R. L. Heinrikson, *J. Biol. Chem.* **1971**, *246*, 4090.
[36] C. A. Rohl, R. L. Baldwin, *Biochemistry* **1997**, *36*, 8435.
[37] P. K. Glasoe, F. A. Long, *J. Phys. Chem.* **1960**, *64*, 188.
[38] D. H. Wu, A. D. Chen, C. S. Johnson, *J. Magn. Reson. Ser. A* **1995**, *115*, 260.
[39] J. A. Jones, D. K. Wilkins, L. J. Smith, C. M. Dobson, *J. Biomol. NMR* **1997**, *10*, 199.
[40] J. Garcia De La Torre, M. L. Huertas, B. Carrasco, *Biophys. J.* **2000**, *78*, 719.

